

1 **Research Article**

2 **Effect of Structural Transformations on Precipitability and**  
3 **Polarity of Red Wine Phenolic Polymers**

4 Ingrid Weilack,<sup>1</sup> Christina Schmitz,<sup>1</sup> James F. Harbertson,<sup>2,3</sup> Fabian Weber<sup>1\*</sup>

5 <sup>1</sup>Institute of Nutritional and Food Sciences, Molecular Food Technology, University of Bonn,  
6 Endenicher Allee 19b, D 53115 Bonn, Germany; <sup>2</sup>Washington State University, 2710 University  
7 Drive, Richland, WA 99354-7224; and <sup>3</sup>Associate Professor of Enology, Washington State  
8 University, Viticulture and Enology Program, School of Food Science.

9 \*Corresponding author (fabian.weber@uni-bonn.de; tel: +49-228-734462; fax: +49-228-734429)

10 This research project was financially supported by the German Ministry of Economics and  
11 Technology (via AiF) and the FEI (Forschungskreis der Ernährungsindustrie e.V., Bonn).  
12 Project AiF 20024 N.

13 Manuscript submitted Oct 20, 2020, revised Jan 19, 2021, accepted Feb 5, 2021

14 This is an open access article distributed under the CC BY license

15 (<https://creativecommons.org/licenses/by/4.0/>).

16 By downloading and/or receiving this article, you agree to the Disclaimer of Warranties and Liability. The  
17 full statement of the Disclaimers is available at [http://www.ajevonline.org/content/proprietary-rights-](http://www.ajevonline.org/content/proprietary-rights-notice-ajev-online)  
18 [notice-ajev-online](http://www.ajevonline.org/content/proprietary-rights-notice-ajev-online). If you do not agree to the Disclaimers, do not download and/or accept this article.

19  
20 **Abstract:** Condensed tannins and polymeric pigments are essential red wine components since  
21 they contribute to color stability, taste, and mouthfeel. Phenolic polymers in red wine consist of  
22 flavan-3-ol monomers as well as anthocyanins and cause the perception of astringency. Due to the  
23 chemical heterogeneity of proanthocyanidin polymers, analytical tools for the determination of the  
24 polymers' structural features are limited. The incorporation of anthocyanins increases the  
25 structural complexity even more and leaves it almost impossible to assess the influence of structure  
26 on the evoked astringency. To obtain a better understanding of the structural diversity of red wine  
27 polymers, this study combines forced aging and the FLASH-fractionation of polyphenolic wine  
28 extracts to reveal the relationship between phenolic polymers and two physicochemical properties,  
29 polarity, and hydrophilicity. Red wine fractions were characterized regarding their polarity,

30 octanol-water partitioning coefficient, protein precipitation assay, UHPLC-MS, and color. Tannin  
31 concentrations in wine decreased during forced aging while the concentrations were constant in  
32 the corresponding extracts, suggesting an alteration of the precipitation behavior. A simultaneous  
33 increase of precipitable polymeric pigments gives rise to the assumption that the incorporation of  
34 anthocyanins into tannin molecules alters the interactions with red wine polysaccharides and  
35 proteins, which results in lower tannin readings. Finding tannins and polymeric pigments in  
36 different FLASH-fractions indicates that precipitability of polymers is affected by the  
37 physicochemical properties, which in turn depend on the degree of polymerization as well as  
38 degree of pigmentation. The results of this study show that red wine astringency and its sub-  
39 qualities may be related to the increase in precipitable polymeric pigments during forced red wine  
40 aging and their putative enhanced interaction with wine polysaccharides and can help to better  
41 understand astringency mechanisms.

42 **Key words:** interactions, physicochemical, pigmentation, polymers, red wine, tannins

## 43 Introduction

44 Phenolic compounds are essential components of wine and anthocyanins and flavan-3-ols  
45 are arguably of utmost importance for red wine quality since they contribute to color and its  
46 stability as well as taste and mouth-feel properties (Cheynier et al. 2006). While monomeric  
47 flavan-3-ols contribute to bitterness, tannins and oligomeric proanthocyanidins are largely  
48 responsible for the perception of astringency (Gawel 1998, Noble 1998). The composition of the  
49 tannins, expressed by the degree of polymerization and galloylation as well as the number of  
50 trihydroxylated monomers, are the driving forces for the intensity and quality of astringency

51 perception, which is explained by a loss of lubrication as a result of polyphenols precipitating  
52 saliva proteins (Noble 1998, de Freitas and Mateus 2001, Vidal et al. 2003, Harbertson et al. 2014).  
53 Anthocyanins determine the color of young red wines and are extracted during wine making. They  
54 have a key role in the modulation of color and mouthfeel properties during red wine aging.

55 Anthocyanins are transformed to more stable pigments which is accompanied by a loss in  
56 wine color density (Bindon et al. 2014). Together with some low molecular wine constituents and  
57 yeast metabolites, anthocyanins can form pyranoanthocyanins (Fulcrand et al. 2006) or can be  
58 incorporated into tannin-like structures. Tannins that incorporate anthocyanins during red wine  
59 aging are designated polymeric pigments (Remy et al. 2000).

60 Chira et al. (2012) reported an age-related decrease of tannin concentrations and mean  
61 degree of polymerization (mDP) accompanied with a decline in perceived astringency. In contrast,  
62 McRae et al. (2012) showed that tannin concentrations were not directly related to wine age and  
63 that tannin size increased during aging indicating that lower astringency ratings of aged wines do  
64 not result solely from lower tannin concentrations and mDPs. Earlier studies (Vidal et al. 2004a,  
65 Weber et al. 2013) suggested that the formation of polymeric pigments found in aged red wine  
66 attenuates astringency. Hence, the incorporation of anthocyanins may affect astringency  
67 perception even more than the concomitant increasing polymer length.

68 Due to similar chemical structures and the chemical heterogeneity of proanthocyanidin  
69 polymer length, sub-unit composition, and constitution, analysis of these phenolics has proved  
70 difficult. Reversed-phase HPLC-DAD-MS is commonly used to identify and quantify low  
71 molecular polyphenols, but this approach is limited regarding tannin analysis since they elute as a  
72 polydisperse hump (Ma et al. 2018). Methods that are utilized to partly characterize red wine

73 polymers include tannin precipitation either by proteins in combination with bisulfite bleaching  
74 (Harbertson et al. 2002, 2003) or polysaccharides (Sarneckis et al. 2006). Acid-catalyzed cleavage  
75 of proanthocyanidins in the presence of nucleophilic agents like phloroglucinol (Kennedy and  
76 Jones 2001) is another approach to assess polymer composition. However, this method showed its  
77 limits when applied to analyze pigmented tannins (Vidal et al. 2004a) and therefore, the manifold  
78 structures of polymeric pigments have not yet been identified. Consequently, the complex  
79 composition and alteration of red wine polymers as well as their impact on astringency perception  
80 remain important issues to be studied.

81 To address this lack of knowledge, this study utilizes normal-phase FLASH-  
82 chromatography to fractionate red wine polyphenols according to their size and polarity. The  
83 fractions were chemically characterized including the determination of their octanol-water  
84 partitioning coefficients ( $K_{OW}$ ) to measure hydrophilicity. A previous study (Merrell et al. 2018)  
85 showed that the  $K_{OW}$  is influenced by tannin composition and red wine maturity. Combining forced  
86 aging and fractionation of polyphenolic wine extracts aims at revealing the relationship between  
87 polymeric pigments as well as tannins and two physicochemical properties. Polarity and  
88 hydrophilicity were investigated to gain a better understanding of the structural diversity of red  
89 wine polymers.

## 90 **Materials and Methods**

### 91 *Materials*

92 Acetic acid, hexane, hydrochloric acid (HCl), potassium bisulfite, and acetonitrile were  
93 purchased from VWR International GmbH (Darmstadt, Germany). Ethanol, bovine serum albumin

94 fraction V, and (+)-Catechin were purchased from Carl Roth (Karlsruhe, Germany). Silica gel 60  
95 Å (particle size 0.063-0.2 mm, 70-230 mesh) and sodium hydroxide were purchased from  
96 Honeywell Fluka (Offenbach, Germany). Urea, maleic acid, ferric chloride, triethanolamine  
97 (TEA), and octanol were purchased from Alfa Aesar (Kandel, Germany). Sodium chloride and  
98 Amberlite XAD7 were purchased from Labochem int. (Heidelberg, Germany) and Sigma-Aldrich  
99 (Darmstadt, Germany), respectively.

#### 100 *Wine samples*

101 Two different commercially available wines were chosen in this study. Six bottles each of  
102 the 2018 Cabernet Sauvignon from the Trapiche winery (Maipú, Mendoza, Argentina) and the  
103 2016 Cabernet Sauvignon from the Salentein winery (Tunuyán, Mendoza, Argentina) were used.  
104 The wines were assessed in advance by FT-IR and in a bench tasting, which verified that both  
105 wines had no considerable differences in their general composition and sensory properties. Two  
106 different wines from two vintages were selected to investigate whether wine phenolic composition  
107 and tannin structures change differently in an older wine compared to a younger wine during forced  
108 aging. The 2018 wine was composed as follows: 13% ethanol by volume, 9 g/L glycerol, pH 3.7,  
109 titratable acidity as 5.9 g/L tartaric acid equivalents, 5 g/L residual sugars, 1935 mg/L catechin  
110 equivalents total phenolic content. The 2016 wine was composed as follows: 13.5% ethanol by  
111 volume, 10 g/L glycerol, pH 3.8, titratable acidity as 5.4 g tartaric acid equivalents/L, 5 g/L residual  
112 sugars, 2117 mg/L catechin equivalents total phenolic content. Apart from the phenolic content,  
113 that was determined according to chapter 2.5, these parameters were obtained using Fourier-  
114 transform mid-infrared spectroscopy, including the appropriate calibration method (WineScan  
115 FT120 Basic, Foss, Hilleroed, Denmark). The total phenolic contents of the wines were not

116 significantly different at  $p \leq 0.05$ . Free and total  $\text{SO}_2$  values were 6 mg/L and 70 mg/L for the 2016  
117 wine and 10 mg/L and 100 mg/L for the 2018 wine determined by titration. The samples were split  
118 into three pairs. Two were kept at 35 °C for three or six weeks and were compared to the non-aged  
119 wines. All bottles were closed with screw caps and the two bottles of each sample were pooled for  
120 all experiments.

### 121 *Solid phase extraction and fractionation of phenolic compounds*

122 To obtain a polyphenol rich extract from the wines, each wine sample was diluted with  
123 water (1:2) and was loaded onto an Amberlite XAD7 column (65 mm x 450 mm; 1.5 L bed  
124 volume), which was previously washed with 250 mL of a 0.1% (w/v) sodium hydroxide solution  
125 and preconditioned with 2 L of water. After elution of the wine, the column was washed with 2 L  
126 of water (1.3 fold of the bed volume) in order to remove sugars and organic acids. The polyphenols  
127 were eluted with approximately 3 L of ethanol acidified with acetic acid (29:1 v/v) at a gravity  
128 flow rate of approximately 10 mL/min. The collected extracts were concentrated using a rotary  
129 evaporator and consecutively lyophilized. The fractionation was conducted on a self-packed silica  
130 gel 60 Å column (36 mm x 460 mm; 0.5 L bed volume) using a low-pressure chromatography  
131 pump (C-605 pump with C-615 pump manager, Büchi Labortechnik GmbH, Essen, Germany).  
132 Isocratic elution involved three solvents: 60% hexane, 40% ethanol (solvent A), ethanol with 1%  
133 formic acid (solvent B), and 50% ethanol (v/v) with 1% formic acid (solvent C). At a flow rate of  
134 90 mL/min the column was first rinsed with solvent C for 10 minutes and then preconditioned with  
135 solvent A for another 10 minutes. Subsequently, 5 mL of extract dissolved in solvent B were loaded  
136 onto the column with a concentration of 75 g/L. Solvent A, B and C were successively applied to  
137 the column for 10 minutes each and changed manually. Elution was monitored at 280 nm and 520

138 nm with a Knauer BlueShadow 50D detector and the ClarityChrom Software (Knauer, Berlin,  
139 Germany). According to the chromatogram obtained at 280 nm, the fractions were manually  
140 combined. After complete elution, solvents were evaporated, and the fractions were lyophilized.  
141 The column was washed with solvent C for 10 minutes. Prior to further analyses, the lyophilized  
142 fractions and extracts were dissolved at concentrations of 2 g/L in a wine-like solution (12%  
143 ethanol by volume, 5 g/L tartaric acid, pH 3.3 adjusted with NaOH).

#### 144 *Spectrophotometric analysis*

145 Absorbance spectra were recorded in undiluted wines and sample solutions between 300  
146 and 800 nm by a Jasco V-730 double-beam spectrophotometer (JASCO Deutschland GmbH,  
147 Pfungstadt, Germany), using a 1 mm path-length glass cuvette (Hellma GmbH & Co. KG,  
148 Müllheim, Germany). After values were corrected to a 10 mm path length cylindrical coordinates  
149 chroma C\* and hue h\* were calculated with the Spectra Manager Ver.2.14G (JASCO Deutschland  
150 GmbH, Pfungstadt, Germany) according to OIV recommendations (OIV 2006).

#### 151 *Chemical characterization*

152 Anthocyanins were analyzed following the protocol reported by Harbertson et al. (2009).  
153 Protein precipitation was combined with bisulfite bleaching to determine tannins and polymeric  
154 pigments (Harbertson et al. 2002, 2003) using a reformulated resuspension buffer (urea 8.3 M, 5%  
155 TEA, pH 7 adjusted with HCl) as published by Harbertson et al. (2015). To quantify total iron  
156 reactive phenolics, an aliquot of the sample is diluted with the previously mentioned resuspension  
157 buffer to a total volume of 875  $\mu$ L and incubated for 10 minutes. Absorbance at 510 nm is  
158 measured before and after addition of 125  $\mu$ L of ferric chloride solution. Tannins and total iron

159 reactive phenolics were expressed as catechin equivalents (CE) according to an external calibration  
160 curve.

#### 161 *Octanol-Water partition coefficient*

162 A volume of 1 mL of the sample solution was thoroughly mixed with 1 mL of octanol and  
163 vortexed for 10 seconds. For faster separation of the phases, the samples were centrifuged at 9,600g  
164 for 10 minutes. Subsequently, an aliquot of both phases was injected into the Shimadzu Nexera  
165 X2 UHPLC-DAD system (two Nexera X2 LC-30AD high-pressure gradient pumps, a Prominence  
166 DGU-20A5R degasser, a Nexera SIL-30AC autosampler (15 °C, injection volume 2 µL), a CTO-  
167 20AC Prominence column oven (40 °C), and a SPD-M20A Prominence diode array detector;  
168 Shimadzu, Kyoto, Japan) using an ACQUITY HSS T3 column (50 mm × 2.1 mm, 1.8 µm; Waters,  
169 Milford, USA). At a flow rate of 0.5 mL/min samples were eluted using the following gradient: 0  
170 min, 50% B; 2 min, 100% B; 3.3 min, 100% B; 4 min, 50% B; 7 min, 50% B, with A being  
171 water/formic acid (97/3; v/v) and B being acetonitrile/formic acid (97/3; v/v). The partitioning  
172 coefficient was formed by the ratio of the samples' total peak area in the octanol phase and the  
173 water phase, respectively, according to the chromatogram at 280 nm.

#### 174 *UHPLC-ESI-MS/MS*

175 UHPLC-MS analysis of the fractions was performed on an Acquity UPLC I-Class system  
176 (Waters, Milford, MA) consisting of a binary pump, an autosampler cooled at 10 °C, a column  
177 oven set at 40 °C, and a diode array detector scanning from 190 to 800 nm. An Acquity HSS-T3  
178 RP18 column (150 × 2.1 mm; 1.8 µm particle size) combined with a precolumn (Acquity UPLC  
179 HSS T3 VanGuard, 100 Å, 2.1 × 5 mm, 1.8 µm), both from Waters (Milford, MA) was used for



180 separation. At a flow rate of 0.5 mL/min analytes were eluted using the following gradient: 0 min,  
181 5% B; 8 min, 10% B; 25 min, 25% B; 26 min, 100% B; 28 min, 100% B; 29 min, 5% B; 31 min,  
182 5% B, with A being water/formic acid (97/3; v/v) and B being acetonitrile/formic acid (97/3; v/v).  
183 The injection volume was 5  $\mu$ L. The UPLC was coupled to a LTQ-XL ion trap mass spectrometer  
184 (Thermo Scientific, Inc., Waltham, MA) equipped with an electrospray interface operating in  
185 positive ion mode for analysis of anthocyanins and anthocyanin derivatives and in negative ion  
186 mode for other polyphenols. For identification, mass spectra were recorded in the range of  $m/z$   
187 120–1500 with three consecutive mass scans ( $MS^2$ , 35% normalized collision energy;  $MS^3$ , 45%  
188 normalized collision energy). The capillary was set at 325 °C with a voltage of 40 V for  $ESI^+$ , and  
189 at 350 °C and a voltage of –44 V for  $ESI^-$ . The source voltage was maintained at 5 and 4 kV,  
190 respectively, at a current of 100  $\mu$ A. The tube lens was adjusted to 70 V for  $ESI^+$  and –105 V for  
191  $ESI^-$ . For quantification, specific  $m/z$  values of 63 polyphenolic compounds were recorded in  
192 single ion monitoring (SIM) measurements using one scan event.

### 193 *Sensory analysis*

194 To determine the effects of alterations of tannin structures on astringency during forced  
195 aging, overall astringency of the wines was evaluated by a panel tasting. The sensory panel was  
196 composed of 14 volunteer judges that participated in three training sessions prior to the final  
197 tasting. The first session was dedicated to the differentiation between astringency, sourness and  
198 bitterness by the panelists who were familiarized with these tastes and sensations. Solutions of  
199 aluminum sulfate (2 g/L), caffeine (1.5 g/L) and tartaric acid (2 g/L) in a Pinot noir wine from  
200 2018 used as basic wine were presented to train astringency, bitterness, and sourness perception.

201 The second session was dedicated to the recognition of various aluminum sulfate concentrations  
202 (0, 0.5, 1 and 2 g/L). Panelists were advised to rank the standard solutions by ascending intensity.  
203 During the third session the panelists were introduced to the intensity scale of the final tasting  
204 which was a structured scale from 1 to 10 for “very low intensity” and “very high intensity”,  
205 respectively. Two astringency standard solutions (0.5 g/L and 3 g/L) were presented and set as  
206 points 3 and 8 of the scale after panel discussion. The final tasting was held in four individual  
207 sessions and three samples were evaluated in each of them. Wine samples were presented in a  
208 balanced random order in coded glasses and were tasted in duplicate. Reference astringency  
209 solutions were provided in each session. The panelists tasted 30 mL of the wine in individual  
210 booths wearing a blindfold. They were advised to neutralize the oral cavity with water and bread  
211 and to wait 3 minutes before tasting the following sample.

### 212 *Statistical analysis*

213 Statistical analysis of the results was performed using XLSTAT (Version 2014.4.06,  
214 AddinSoft Technologies, Paris, France). For pairwise comparisons, an ANOVA with a selected  
215 significance level of  $p < 0.05$  was used.

## 216 **Results**

### 217 *Wine samples and storage*

218 The two wines chosen for this study presented a similar initial composition and were stored  
219 at elevated temperature to accelerate reactions normally occurring during red wine aging. Two  
220 bottles of each wine were subjected to forced aging for three or six weeks. The results of the FT-  
221 IR analysis revealed only negligible changes in the wines' general composition after storage. The

222 color assessed by the CIELab parameters hue and chroma (Table 1), showed that the 2018 wines  
223 exhibited greater color intensities than the 2016 samples. In contrast to the rather high  $\Delta E$  values  
224 between fresh and stored samples of 4.66 and 8.93 for the 2016 and 2018 wines, respectively, the  
225 color differences were hardly perceptible. The higher  $\Delta E$  value of the 2018 wines may be explained  
226 by the faster loss of anthocyanins in younger wines due to the exponential decline of anthocyanins  
227 during aging (McRae et al. 2012).

228         Since color intensity is correlated with anthocyanin concentration and red wine maturity,  
229 the loss of color is consistent with the fast decline of anthocyanin concentrations during storage  
230 (Figure 1A). This development can be explained by the degradation, conversion, and incorporation  
231 of anthocyanins into pyranoanthocyanins and polymeric pigments, respectively. Figures 1B and  
232 1C indicate higher proportions of polymeric pigments in the 2016 wines compared to the 2018  
233 samples, whereby both contain more non-precipitable polymeric pigments (PP) than precipitable  
234 PP. While the proportion of precipitable PP is increasing in both samples, the amount of non-  
235 precipitable PP is increasing only in the 2018 wine. In the 2016 wine, non-precipitable PP  
236 concentration leveled, whereas in the 2018 wine, the non-precipitable PP concentration increased.  
237 While concentrations of precipitable PP increased, tannin concentrations decreased in the wine  
238 samples (Figure 1).

239         Since the wines did not show considerable differences in terms of sourness and bitterness,  
240 which was also proven by the FT-IR data, only wine astringency was further assessed in the  
241 sensory analysis. The sensory evaluation of the perceived astringency revealed that the 2016 wine  
242 appears to induce higher but still moderate astringency (Table 2). A four-way ANOVA of the

243 astringency rating including vintage, storage, panelist, and replicate is presented in Supplemental  
244 Table 1. The astringency of the wines slightly declined which is in line with the findings for tannin  
245 concentrations (Figure 1D). Interestingly, the astringency of the 3 weeks stored 2018 sample  
246 dropped to 3.5 but increased during another 3 weeks of storage. This coincides only partially with  
247 the tannin concentrations as tannin concentration declined constantly over time in the 2018 wine.

#### 248 *Isolation of a polyphenol rich extract and fractionation using silica gel*

249 The yields of the polyphenol rich extracts obtained by solid phase extraction using  
250 Amberlite XAD7 as solid phase were  $3.6 \pm 0.1$  g/L for the 2018 wines and  $4.1 \pm 0.1$  g/L for the 2016  
251 wines. For every wine sample, the low-pressure fractionation on silica gel was repeated 6 to 8  
252 times to produce enough material for the following analyses. The separation with silica gel  
253 primarily works on size exclusion, but hydrogen bonding between the phenolics and the silanol  
254 groups also plays an important role. The ternary isocratic separation of the injected extracts  
255 generated three fractions and the corresponding yields, and the distribution are given in Table 3.  
256 The elution of the fractions was monitored at 280 and 520 nm.

#### 257 *Composition of the FLASH fractions*

258 Table 1 presents the color metrics recorded for the fractions of all wine samples. With  
259 chroma values of 13 to 16 and a color hue of around 70, fractions 1 had a light orange to yellow  
260 coloration indicating a limited amount of red pigments. Having color hues of 28 and 35 each  
261 fraction 2 and 3 of the 2018 wine were closer to a blueish red color than fraction 2 and 3 of the  
262 2016 wine with values of 37 and 41, respectively.

263           The results of the protein precipitation assay (Figure 2A) show that the highest number of  
264 anthocyanins was found in fraction 2 of the 2018 wine. In all fractions, the amount of non-  
265 precipitable PP (Figure 2B) is higher than that of precipitable PP (Figure 2C) and tannins were  
266 only found in fractions 2 and 3. Tannins, polymeric pigments, and monomeric anthocyanins are  
267 absent in fraction 1, suggesting that fraction 1 is mainly composed of non-polar and non-phenolic  
268 substances.

269           Figure 3 presents the octanol water partitioning coefficients ( $K_{ow}$ ) of the fractions. A  $K_{ow}$   
270 higher than 1 implies that the fraction is lipophilic, while values below 1 express the hydrophilicity  
271 of the contained compounds. The  $K_{ow}$  of the fractions follows the elution gradient of the FLASH  
272 separation as expected, where fraction 1 showed hydrophobic properties, while fractions 2 and 3  
273 are both hydrophilic. The highest hydrophilicity is found in fraction 3 of both vintages. Merrell et  
274 al. (2018) determined the octanol water partitioning coefficients of young and aged Cabernet  
275 Sauvignon wines and defined coefficients of around 0.19 for young wines. This is comparable to  
276 the values found in this study for the wine extracts (Figure 3A).

277           The results of the UHPLC-MS analyses show that fraction 1 mainly contains gallic acid,  
278 monomeric flavan-3-ols, hydroxycinnamic acids and oligomeric procyanidins, whereas malvidin-  
279 3-*O*-glucoside is the main compound in fractions 2 and 3 (Supplemental Table 2 and 3). In  
280 agreement with the color and the precipitation assay, fraction 1 is characterized by the absence of  
281 anthocyanins and their derivatives.

282

283 *Changes in the fractions during wine storage*

284           The storage of the wines did not change the quantitative proportions of the fractions.  
285 Anthocyanins in fractions 2 and 3 declined in both vintages. The decrease in anthocyanins does  
286 not lead to a loss in color intensity (chroma), but goes along with a change in hue which indicates  
287 structural changes of pigments rather than a mere loss. Non-precipitable PP (Figure 2B) of the  
288 2018 wine increased in fraction 2 and decreased in fraction 3. Since a less polar solvent elutes  
289 fraction 2, these developments of non-precipitable PP also indicate structural transformations of  
290 molecules, which correspond with declining polarities. In the 2016 wine, non-precipitable PP  
291 concentrations remained constant in both fractions. In fractions 2 and 3, precipitable PP (Figure  
292 2C) increased during storage. No changes in tannin concentrations were detected except in fraction  
293 2 of the 2016 wine, which showed a slight decrease indicating that the amount of less polar tannins  
294 of the 2016 wine decreased over time.

295           As a result of lower concentrations in polymeric pigments, the color of fraction 3 of the  
296 2018 wine changed the most while the color of the other fractions (Table 1) was rather constant.  
297 It is apparent that the hydrophilicity of the fractions changed significantly during storage, however  
298 alterations are rather small with only fraction 3 of the 2018 wine undergoing considerable changes  
299 (Figure 3). Fraction 1 of the 2016 wine becomes more hydrophilic while fraction 1 of the 2018  
300 wine shows higher hydrophobicity after storage. In fraction 2 of the 2016 wine and fraction 3 of  
301 the 2018 wine the hydrophilicity is increasing, whereas in fraction 3 of the 2016 wine and fraction  
302 2 of the 2018 wine at the end of the 6 weeks storage no change was detected. Nevertheless, a rise

303 and a decrease of water solubility in fraction 3 of the 2016 wine and fraction 2 of the 2018 wine,  
304 respectively, occurred after 3 weeks.

305 In contrast to the anthocyanin concentrations, the UHPLC-MS results show no changes in  
306 the concentration of anthocyanin-derived pigments like pyranoanthocyanins or anthocyanin-  
307 flavanol oligomers (Supplemental Table 2 and 3). Likewise, monomeric flavanols, benzoic acids,  
308 hydroxycinnamic acids, flavanol dimers and trimers did not decrease.

### 309 Discussion

310 This study was conducted to gain a deeper understanding of structural transformations of  
311 polyphenols occurring during forced red wine aging and their effects on astringency perception.  
312 Earlier studies (Boselli et al. 2004, Landon et al. 2008, Chira et al. 2011) associated red wine  
313 astringency with tannin concentrations as well as the vintage of the wines. Accordingly, the  
314 astringency of the 2018 wine was expected to be higher than that of the 2016 wine, and the wines  
315 were expected to decrease in astringency during forced aging; neither of which was actually  
316 observed (Table 2). This indicates that astringency is not only influenced by tannin concentrations  
317 but also by structural and compositional differences (Gawel 1998) like the degree of  
318 polymerization (Chira et al. 2012) and the composition of tannin sub-units, in particular their  
319 degree of galloylation and trihydroxylation on the B-ring (Vidal et al. 2003). According to Vidal  
320 et al. (2003) roughness of astringency increases with proceeding galloylation and decreases with  
321 the number of epigallocatechin subunits. To compare tannin concentration in the wines and  
322 extracts, the values obtained for the extracts were referenced to the corresponding volume of the  
323 wine considering the respective yield (Table 3). In contrast to the results obtained for the wines,

324 significantly higher tannin concentrations and no significant changes of tannin concentrations were  
325 found in the XAD7 extracts of the corresponding wines. These differences may be explained by  
326 interactions of the tannins with wine polysaccharides that are eliminated by the extraction  
327 procedure. The polysaccharides can form complexes with the tannins leading to an impaired  
328 precipitability with the BSA (Mateus et al. 2004) used for tannin quantification which results in  
329 lower tannin readings. Since the differences in tannin concentrations between wines and extracts  
330 increased, these interactions appear to become more pronounced when the wine is subjected to  
331 forced aging probably due to structural changes of the tannins. Precipitable PPs can be regarded  
332 as pigmented tannins since they are part of the tannin fraction determined after precipitation with  
333 BSA. The results show increasing precipitable PP ratios combined with decreasing or constant  
334 tannin levels indicating a progressive incorporation of anthocyanins into tannin molecules.  
335 Sommer et al. (2016) investigated the haze formation in red wines when treated with  
336 carboxymethyl cellulose (CMC). They found that CMC forms haze with wine proteins rather than  
337 with tannins and proposed a protein-bridged reaction between anthocyanins and CMC that leads  
338 to their precipitation. Accordingly, the incorporation of anthocyanins into tannin molecules  
339 changes the interaction between tannin sub-units and polysaccharides as well as proteins  
340 camouflaging them from analysis. Polysaccharides may also interact directly with BSA (de Freitas  
341 et al. 2003), which is used for tannin precipitation and might be another reason for the  
342 underestimation of tannins in wine samples. Astringency perception is also affected by wine  
343 polysaccharides that interact with red wine tannins and salivary proteins (Vidal et al. 2004b ,  
344 Watrelot et al. 2017). Panelists were only requested to rate the overall astringency intensity that  
345 was compared to the drying mouthfeel evoked by aluminum sulfate. Future research should look



346 at the perception of different astringency sub-qualities to investigate whether the decrease of  
347 astringency rather represents a change in sub-qualities towards a less harsh mouthfeel. These  
348 results show that the tannin concentration may not be the only factor that should be considered for  
349 an evaluation of astringency and the sensory quality of the wine in general. Weber et al. (2013)  
350 showed that gel permeation chromatography fractions containing the highest number of polymeric  
351 pigments and rather small tannin concentrations elicited the lowest astringency as well as green  
352 and dry tannins intensity. A continuously increasing precipitable PP/tannin ratio of the wines may  
353 have favored the perception of a softer astringency.

354 The mechanism of astringency perception is based on tannin-protein interactions leading to  
355 insoluble precipitates, increasing friction and a loss of lubrication in the oral cavity (Baxter et al.  
356 1997). Charlton et al. (2002) proposed a model for protein precipitation that is initially driven by  
357 hydrophobic interactions between the proline residues of proline-rich proteins and the aromatic  
358 flavonoid rings. These soluble aggregates are further stabilized through hydrogen bonding leading  
359 to cross linked tannin-protein complexes and their precipitation, suggesting that hydrophilicity is  
360 an important factor determining the astringency of distinct compounds.

361 The ratio of the concentration of lipophilic to hydrophilic compounds in the fractions is  
362 reflected by the octanol water partitioning coefficient ( $K_{OW}$ ). The generally higher anthocyanin  
363 concentrations in fraction 2 of all samples raised the expectation to observe higher hydrophilicities  
364 of this fraction compared with fraction 3. Since this was not the case, other compounds, like  
365 polymeric pigments and tannins, apparently contribute more to the overall hydrophilicity of the  
366 fractions. Hagerman et al. (1998) investigated the effect of growing tannin polymer lengths on the  
367 precipitability and the  $K_{OW}$ . They stated that tannins with higher degrees of polymerization

368 exhibited lower octanol water partitioning coefficients compared to their corresponding flavan-3-  
369 ol subunits. Hence, a higher degree of polymerization results in higher hydrophilic properties and  
370 precipitability. The hydrophobic character of fractions 1 is the result of the presence of monomeric  
371 flavan-3-ols, oligomeric procyanidins as well as benzoic and hydroxycinnamic acids.

372 The leveling concentrations of non-precipitable PP in fractions 2 and 3 of the 2016 wine lead  
373 to the assumption that the wines reached a maximum of non-precipitable PP which was already  
374 reported by Merrell et al. (2018) and may have two explanations. First, the formation and  
375 degradation processes of non-precipitable PP reached an equilibrium or, second, the formation of  
376 polymeric pigments in the older red wine that was subjected to forced aging favors the  
377 development of high molecular pigments that are not included into the non-precipitable PP  
378 measurement. Harbertson et al. (2014) showed that precipitation with BSA increases with polymer  
379 size of the tannins indicating that polymeric pigments that are resistant against SO<sub>2</sub> bleaching and  
380 that are not precipitated with BSA include oligomeric anthocyanin adducts as well as  
381 pyranoanthocyanins. The UHPLC-MS results show no considerable changes in the concentration  
382 of pyranoanthocyanins and anthocyanin-flavanol dimers (Supplemental Table 2 and 3). Hence, the  
383 protein precipitation assay indicates that anthocyanins are incorporated into existing polymeric  
384 structures to form polymeric pigments rather than forming new oligomeric pigments that grow in  
385 size. This is supported by earlier studies (Haslam 1980, Salas et al. 2003, Salas et al. 2004) that  
386 demonstrated that direct adducts of tannins and anthocyanins are formed after the preceding acid-  
387 catalyzed cleavage of procyanidins. The products formed during this reaction may still be regarded  
388 as polymeric structures although they might be of lower molecular weight due to the breakdown  
389 process.

390 The decline of tannins in fraction 2 of the 2016 wine together with a rise of precipitable PP  
391 results in the increase of hydrophilicity. This indicates that tannins initially found in fraction 2 of  
392 the 2016 wine are rather small and, thus, non-polar and hydrophobic, whereas the proceeding  
393 incorporation of anthocyanins during forced aging leads to more water soluble polymeric pigments  
394 (Singleton and Trousdale 1992, Merrell et al. 2018). Since the tannin concentration of fraction 3  
395 of the 2016 wine remains constant, the corresponding partitioning coefficients follow the  
396 developments of precipitable PP, showing that fraction 3 of the 2016 wine contains large and polar  
397 tannins that were progressively pigmented during storage. In the 2018 wines, tannin concentrations  
398 in fractions 2 and 3 show no changes over time and accordingly, hydrophilicity seems to be  
399 affected by the compositional changes of precipitable PP and non-precipitable PP. As the  
400 determination of polymeric pigments is based on their absorption at 520 nm, the protein-  
401 precipitation assay does not distinguish between polymers of different intramolecular  
402 compositions (Weber et al. 2013). Hence, no conclusion can be drawn about the exact size of the  
403 molecules and the proportion of anthocyanins incorporated. Weber et al. (2013) examined the  
404 chemical composition of red wine polymers obtained by gel permeation chromatography that is  
405 based on the separation of molecules due to their size and polarity. Combining several analytical  
406 techniques, they stated that early eluting fractions were composed of large and less pigmented  
407 polymers. Further retention on the column eluted polymers with decreasing molecular size and  
408 increasing anthocyanin incorporation followed by less pigmented proanthocyanidin-like  
409 oligomers. Together with the results of the present study, the changes in hydrophilicity as well as  
410 the distribution of polymeric pigments between the fractions visualize the compositional  
411 transformations of red wine polymers. The hydrophilicity of fraction 2 of the 2018 wine decreased

412 during the first 3 weeks while the amount of precipitable PP increased. Because fraction 2 contains  
413 less polar and smaller polymers compared to fraction 3, this suggests an increase in the amount of  
414 smaller precipitable PP rather than an increase in the proportion of incorporated anthocyanins, i.e.  
415 the degree of pigmentation.

416 In contrast, the increase in hydrophilicity after 6 weeks resulted from the increase in non-  
417 precipitable PP or rather the augmented pigmentation of non-precipitable PP. The progressive  
418 increase in hydrophilicity of fraction 3 of the 2018 wine is caused by the ongoing new formation  
419 of larger precipitable PP or the continuous pigmentation of already existing large precipitable PP,  
420 and the simultaneous decrease of smaller non-precipitable PP that are less pigmented.

421 The different sub-qualities of astringency perception are explained by the varying  
422 manifestation of the physico-chemical interactions between tannins and proteins, which are  
423 specific and dependent on the molecular weight, the 3D structure and the water-solubility of  
424 tannins, that is, according to Haslam (1996), one of the main factors for tannin complexation  
425 (Simon et al. 2003). Being of a certain size, polyphenols can act as multidentate ligands binding  
426 more than one site of the protein (de Freitas and Mateus 2001) leading to the formation of protein-  
427 tannin networks and eventually precipitation (Cala et al. 2010). The formation of such networks  
428 and resulting astringent sensations were shown to be influenced by stereochemistry and  
429 conformation of procyanidins, because intramolecular stacking hinders the development of  
430 protein-tannin aggregates (Cala et al. 2010, Quijada-Morín et al. 2012). An earlier study (McRae  
431 et al. 2010) showed that the interactions between red wine tannins and a prolin-rich peptide  
432 changed with wine age towards less pronounced hydrophobic interactions. The authors attribute  
433 this to the change of tannin structures, like the incorporation of anthocyanins.

434 In 2013, McRae et al. showed that tannins obtained by liquid liquid extraction with butanol  
435 were smaller in size, more hydrophobic and comprise more red pigments than the aqueous  
436 fractions, which was inversely correlated with the perceived astringency. The findings of McRae  
437 et al. (2013), the results published by Weber et al. (2013), and the results of the present study argue  
438 for the concept of pigmented tannins being less astringent than non-pigmented tannins.  
439 Accordingly, a higher degree of pigmentation is not necessarily resulting in lower hydrophobicity  
440 since other structural features also contribute to the overall hydrophobicity of the tannins. The  
441 higher hydrophobicity of the butanol tannins may be due to a greater oxidation and an increased  
442 amount of intramolecular bonds possibly leading to a reduced number of binding sites, hence, a  
443 reduced astringency (McRae et al. 2013). The interim decline of astringency of the 2018 wine  
444 stored for 3 weeks might be the consequence of the considerably higher non-precipitable PP in  
445 fraction 2 and the increase in hydrophobicity of this fraction at this point of forced aging, while  
446 the further alterations of the tannins lead to an increase in astringency after 6 weeks of storage.

447 Finding tannins, PP in both, fraction 2 and fraction 3, indicates that not only the size of these  
448 polymers is important for their protein precipitability. It is affected by the physicochemical  
449 properties, which in turn depend on the size of tannin molecules and the ratio of incorporated  
450 anthocyanins, among others. However, it has still to be investigated how the elongation of  
451 polymers by anthocyanins as well as flavanols influences the protein precipitability.

## 452 Conclusion

453 The present results reveal that a wide structural variety of pigments can be found within the  
454 classification of polymeric pigments into two categories. This variety is based on the differences

455 of sub-units as well as chain length and ratio of incorporated anthocyanins and leads to polymers  
456 of different physicochemical properties that can be visualized by the octanol-water partitioning  
457 coefficient and the FLASH fractionation. The change of polarity of polymeric pigments in turn  
458 alters their ability to interact with wine polysaccharides and saliva proteins. Since the presumed  
459 proceeding incorporation of anthocyanins into tannin molecules, which can be assumed by the  
460 presented increase in precipitable PP, appears to reduce the measurability of precipitable tannins  
461 during forced aging, a special role may be assigned to the interactions of precipitable PP with  
462 polysaccharides and proteins. The formation of precipitable PPs during forced red wine aging and  
463 their putative enhanced interactions with wine polysaccharides obviously play a key role in the  
464 perception of red wine astringency. In particular, the perception of different sub-qualities of  
465 astringency seems to be related to the proportion of precipitable PP and polysaccharides, which  
466 needs to be addressed in the course of continuing research.

#### 467 **Literature Cited**

- 468 Adams DO, Harbertson JF, Picciotto EA. 2004. Fractionation of red wine polymeric pigments by protein  
469 precipitation and bisulfite bleaching. *In* Red Wine Color. AL Waterhouse and JA Kennedy (eds.),  
470 pp. 275–288. Am. Chem. Soc., Washington, DC.
- 471 Baxter NJ, Lilley TH, Haslam E, Williamson MP. 1997. Multiple interactions between polyphenols and a  
472 salivary proline-rich protein repeat result in complexation and precipitation. *Biochemistry*  
473 36:5566–5577.
- 474 Bindon KA, McCarthy MG, Smith PA. 2014. Development of wine colour and non-bleachable pigments  
475 during the fermentation and ageing of (*Vitis vinifera* L. cv.) Cabernet Sauvignon wines differing in  
476 anthocyanin and tannin concentration. *LWT* 59:923–932.
- 477 Boselli E, Boulton RB, Thorngate JH, Frega NG. 2004. Chemical and sensory characterization of DOC red  
478 wines from Marche (Italy) related to vintage and grape cultivars. *J. Agric. Food Chem.* 52:3843–  
479 3854.

- 480 Cala O, Pinaud N, Simon C, Fouquet E, Laguerre M, Dufourc EJ, Pianet I. 2010. NMR and molecular  
481 modeling of wine tannins binding to saliva proteins: revisiting astringency from molecular and  
482 colloidal prospects. *FASEB J.* 24:4281–4290.
- 483 Charlton AJ, Baxter NJ, Khan ML, Moir AJG, Haslam E, Davies AP, Williamson MP. 2002.  
484 Polyphenol/peptide binding and precipitation. *J. Agric. Food Chem.* 50:1593–1601.
- 485 Cheynier V, Dueñas-Paton M, Salas E, Maury C, Souquet J-M, Sarni-Manchado P, Fulcrand H. 2006.  
486 Structure and properties of wine Pigments and tannins. *Am J Enol Vitic* 57:298–305.
- 487 Chira K, Pacella N, Jourdes M, Teissedre P-L. 2011. Chemical and sensory evaluation of Bordeaux wines  
488 (Cabernet-Sauvignon and Merlot) and correlation with wine age. *Food Chem.* 126:1971–1977.
- 489 Chira K, Jourdes M, Teissedre P-L. 2012. Cabernet sauvignon red wine astringency quality control by  
490 tannin characterization and polymerization during storage. *Eur. Food Res. and Technol.* 234:253–  
491 261.
- 492 de Freitas V, Mateus N. 2001. Structural features of procyanidin interactions with salivary proteins. *J.*  
493 *Agric. Food Chem.* 49:940–945.
- 494 de Freitas V, Carvalho E, Mateus N. 2003. Study of carbohydrate influence on protein–tannin aggregation  
495 by nephelometry. *Food Chem.* 81:503–509.
- 496 Fulcrand H, Dueñas M, Salas E, Cheynier V. 2006. Phenolic reactions during winemaking and aging. *Am*  
497 *J Enol Vitic* 57:289–297.
- 498 Gawel R. 1998. Red wine astringency: A review. *Aust. J. Grape Wine Res.* 4:74–95.
- 499 Hagerman AE, Rice ME, Ritchard NT. 1998. Mechanisms of protein precipitation for two tannins,  
500 pentagalloyl glucose and epicatechin 16 (4→8) catechin (procyanidin). *J. Agric. Food Chem.*  
501 46:2590–2595.
- 502 Harbertson JF, Kennedy JA, Adams DO. 2002. Tannin in skins and seeds of Cabernet Sauvignon, Syrah,  
503 and Pinot noir berries during ripening. *Am J Enol Vitic* 53:54–59.
- 504 Harbertson JF, Picciotto EA, Adams DO. 2003. Measurement of polymeric pigments in grape berry extracts  
505 and wines using a protein precipitation assay combined with bisulfite bleaching. *Am J Enol Vitic*  
506 54:301–306.
- 507 Harbertson JF, Mireles MS, Harwood ED, Weller KM, Ross CF. 2009. Chemical and sensory effects of  
508 saignée, water addition, and extended maceration on high Brix must. *Am J Enol Vitic* 60:450–460.
- 509 Harbertson JF, Kilmister RL, Kelm MA, Downey MO. 2014. Impact of condensed tannin size as individual  
510 and mixed polymers on bovine serum albumin precipitation. *Food Chem.* 160:16–21.
- 511 Harbertson JF, Mireles M, Yu Y. 2015. Improvement of BSA tannin precipitation assay by reformulation  
512 of resuspension buffer. *Am J Enol Vitic* 66:95–99.
- 513 Haslam E. 1980. In vino veritas: Oligomeric procyanidins and the ageing of red wines. *Phytochemistry*  
514 19:2577–2582.

- 515 Haslam E. 1996. Natural polyphenols (vegetable tannins) as drugs: Possible modes of action. *J. Nat. Prod.*  
516 59:205–215.
- 517 Kennedy JA, Jones GP. 2001. Analysis of proanthocyanidin cleavage products following acid-catalysis in  
518 the presence of excess phloroglucinol. *J. Agric. Food Chem.* 49:1740–1746.
- 519 Landon JL, Weller K, Harbertson JF, Ross CF. 2008. Chemical and sensory evaluation of astringency in  
520 Washington State red wines. *Am J Enol Vitic* 59:153–158.
- 521 Ma W, Waffo-Tégou P, Alessandra Passignoni M, Jourdes M, Teissedre P-L. 2018. New insight into the  
522 unresolved HPLC broad peak of Cabernet Sauvignon grape seed polymeric tannins by combining  
523 CPC and Q-ToF approaches. *Food Chem.* 249:168–175.
- 524 Mateus N, Carvalho E, Luís C, de Freitas V. 2004. Influence of the tannin structure on the disruption effect  
525 of carbohydrates on protein–tannin aggregates. *Anal. Chim. Acta* 513:135–140.
- 526 McRae JM, Falconer RJ, Kennedy JA. 2010. Thermodynamics of grape and wine tannin interaction with  
527 polyproline: Implications for red wine astringency. *J. Agric. Food Chem.* 58:12510–12518.
- 528 McRae JM, Damberg RG, Kassara S, Parker M, Jeffery DW, Herderich MJ, Smith PA. 2012. Phenolic  
529 compositions of 50 and 30 year sequences of Australian red wines: The impact of wine age. *J.*  
530 *Agric. Food Chem.* 60:10093–10102.
- 531 McRae JM, Schulkin A, Kassara S, Holt HE, Smith PA. 2013. Sensory properties of wine tannin fractions:  
532 implications for in-mouth sensory properties. *J. Agric. Food Chem.* 61:719–727.
- 533 Merrell CP, Larsen RC, Harbertson JF. 2018. Effects of berry maturity and wine alcohol on phenolic content  
534 during winemaking and aging. *Am J Enol Vitic* 69:1–11.
- 535 Noble AC. 1998. Why do wines taste bitter and feel astringent? *In* *Chemistry of Wine Flavor*. AL  
536 Waterhouse and SE Ebeler (eds.), pp. 156–165. Am. Chem. Soc., Washington, DC.
- 537 OIV. 2006. Determination of chromatic characteristics according to CIELab. Resolution Oeno 1/2006 OIV,  
538 Paris, France.
- 539 Quijada-Morín N, Regueiro J, Simal-Gándara J, Tomás E, Rivas-Gonzalo JC, Escribano-Bailón MT. 2012.  
540 Relationship between the sensory-determined astringency and the flavanolic composition of red  
541 wines. *J. Agric. Food Chem.* 60:12355–12361.
- 542 Remy S, Fulcrand H, Labarbe B, Cheynier V, Moutounet M. 2000. First confirmation in red wine of  
543 products resulting from direct anthocyanin–tannin reactions. *J. Sci. Food Agric.* 80:745–751.
- 544 Salas E, Fulcrand H, Meudec E, Cheynier V. 2003. Reactions of anthocyanins and tannins in model  
545 solutions. *J. Agric. Food Chem.* 51:7951–7961.
- 546 Salas E, Atanasova V, Poncet-Legrand C, Meudec E, Mazaure JP, Cheynier V. 2004. Demonstration of  
547 the occurrence of flavanol–anthocyanin adducts in wine and in model solutions. *Anal. Chim. Acta*  
548 513:325–332.



- 549 Sarneckis CJ, Damberg RG, Jones P, Mercurio M, Herderich MJ, Smith PA. 2006. Quantification of  
550 condensed tannins by precipitation with methyl cellulose: development and validation of an  
551 optimised tool for grape and wine analysis. *Aust. J. Grape Wine Res.* 12:39–49.
- 552 Simon C, Barathieu K, Laguerre M, Schmitter J-M, Fouquet E, Pianet I, Dufourc EJ. 2003. Three-  
553 Dimensional structure and dynamics of wine tannin–saliva protein complexes. A multitechnique  
554 approach. *Biochemistry* 42:10385–10395.
- 555 Singleton VL, Trousdale EK. 1992. Anthocyanin-tannin interactions explaining differences in polymeric  
556 phenols between white and red wines. *Am J Enol Vitic* 43:63–70.
- 557 Sommer S, Dickescheid C, Harbertson JF, Fischer U, Cohen SD. 2016. Rationale for haze formation after  
558 carboxymethyl cellulose (CMC) addition to red wine. *J. Agric. Food Chem.* 64:6879–6887.
- 559 Vidal S, Francis L, Guyot S, Marnet N, Kwiatkowski M, Gawel R, Cheynier V, Waters EJ. 2003. The  
560 mouth-feel properties of grape and apple proanthocyanidins in a wine-like medium. *J. Sci. Food  
561 Agric.* 83:564–573.
- 562 Vidal S, Francis L, Noble A, Kwiatkowski M, Cheynier V, Waters E. 2004a. Taste and mouth-feel  
563 properties of different types of tannin-like polyphenolic compounds and anthocyanins in wine.  
564 *Anal. Chim. Acta* 513:57–65.
- 565 Vidal S, Francis L, Williams P, Kwiatkowski M, Gawel R, Cheynier V, Waters E. 2004b. The mouth-feel  
566 properties of polysaccharides and anthocyanins in a wine like medium. *Food Chem.* 85:519–525.
- 567 Watrelot AA, Schulz DL, Kennedy JA. 2017. Wine polysaccharides influence tannin-protein interactions.  
568 *Food Hydrocoll.* 63:571–579.
- 569 Weber F, Greve K, Durner D, Fischer U, Winterhalter P. 2013. Sensory and chemical characterization of  
570 phenolic polymers from red wine obtained by gel permeation chromatography. *Am J Enol Vitic*  
571 64:15–25.
- 572

**Table 1** CIELab parameters of Cabernet Sauvignon wines and silica gel fractions at the various stages of storage at 35°C.

Sample	weeks	Wine		Fraction 1		Fraction 2		Fraction 3	
		h°	C*	h°	C*	h°	C*	h°	C*
2016	0	14.97	29.12	69.82	15.21	36.23	53.21	40.39	45.44
	3	15.88	23.94	72.84	15.96	37.36	53.08	40.67	47.99
	6	16.13	24.62	72.84	13.80	37.81	52.22	42.75	46.86
2018	0	20.17	38.88	70.18	14.52	27.36	50.47	32.56	47.08
	3	17.6	30.1	71.16	13.09	28.44	51.15	35.19	41.75
	6	18.07	30.54	71.49	13.60	29.54	51.33	37.25	42.29

**Table 2** Astringency ratings (left) of Cabernet Sauvignon wines at the various stages of storage at 35°C (means presented with standard deviation; n = 14;). Means within columns and between tannin concentrations having the same letters are not significantly different at  $p \leq 0.05$ . Tannin concentrations of the wines and the corresponding extracts (right); means presented with standard deviation; n = 3; Concentrations with different capital letters are significantly different between the wines and the extracts ( $p \leq 0.05$ ).

Sample	Weeks	Wine		Extract
		Astringency	Tannins (mg/L CE)	Tannins (mg/L CE)
2016	0	6.52 ± 1.50 a	692.05 ± 3.24 B	732.72 ± 6.67 A
	3	6.27 ± 1.86 ab	669.48 ± 20.68 BC	729.49 ± 11.56 A
	6	5.46 ± 2.48 ab	654.98 ± 12.39 C	727.63 ± 7.38 A
2018	0	5.50 ± 2.13 ab	607.66 ± 4.15 D	587.15 ± 2.12 D
	3	3.56 ± 1.09 c	535.39 ± 18.45 E	585.92 ± 5.29 D
	6	4.53 ± 1.47 bc	508.49 ± 8.64 E	605.81 ± 2.61 D

**Table 3** Yields and proportions (in parentheses) of silica gel chromatography fractions of Cabernet Sauvignon XAD7 extracts after storage at 35°C (means presented with standard deviation; n = 6-8).

Sample	2016			2018		
	Yield (mg/g) (Proportion (%))					
Weeks	0	3	6	0	3	6
F1	130.2 ± 29.4	162.2 ± 0.8	162.1 ± 3.7	154.0 ± 45.1	158.7 ± 39.7	145.9 ± 44.5
	(21.0 ± 4.7)	(25.1 ± 0.2)	(24.9 ± 0.6)	(24.8 ± 7.2)	(23.4 ± 5.9)	(21.7 ± 6.6)
F2	396.8 ± 6.8	368.4 ± 31.6	378.7 ± 12.4	421.2 ± 29.1	450.4 ± 2.3	451.1 ± 71.2
	(64.0 ± 1.2)	(57.0 ± 4.5)	(58.1 ± 1.9)	(67.7 ± 4.7)	(66.4 ± 0.3)	(67.1 ± 10.6)
F3	93.4 ± 10.8	114.6 ± 39.9	112.6 ± 8.4	48.3 ± 17.8	70.1 ± 19.4	75.7 ± 20.7
	(15.1 ± 3.8)	(17.7 ± 5.8)	(17.3 ± 1.3)	(7.8 ± 2.9)	(10.3 ± 2.9)	(11.3 ± 3.1)

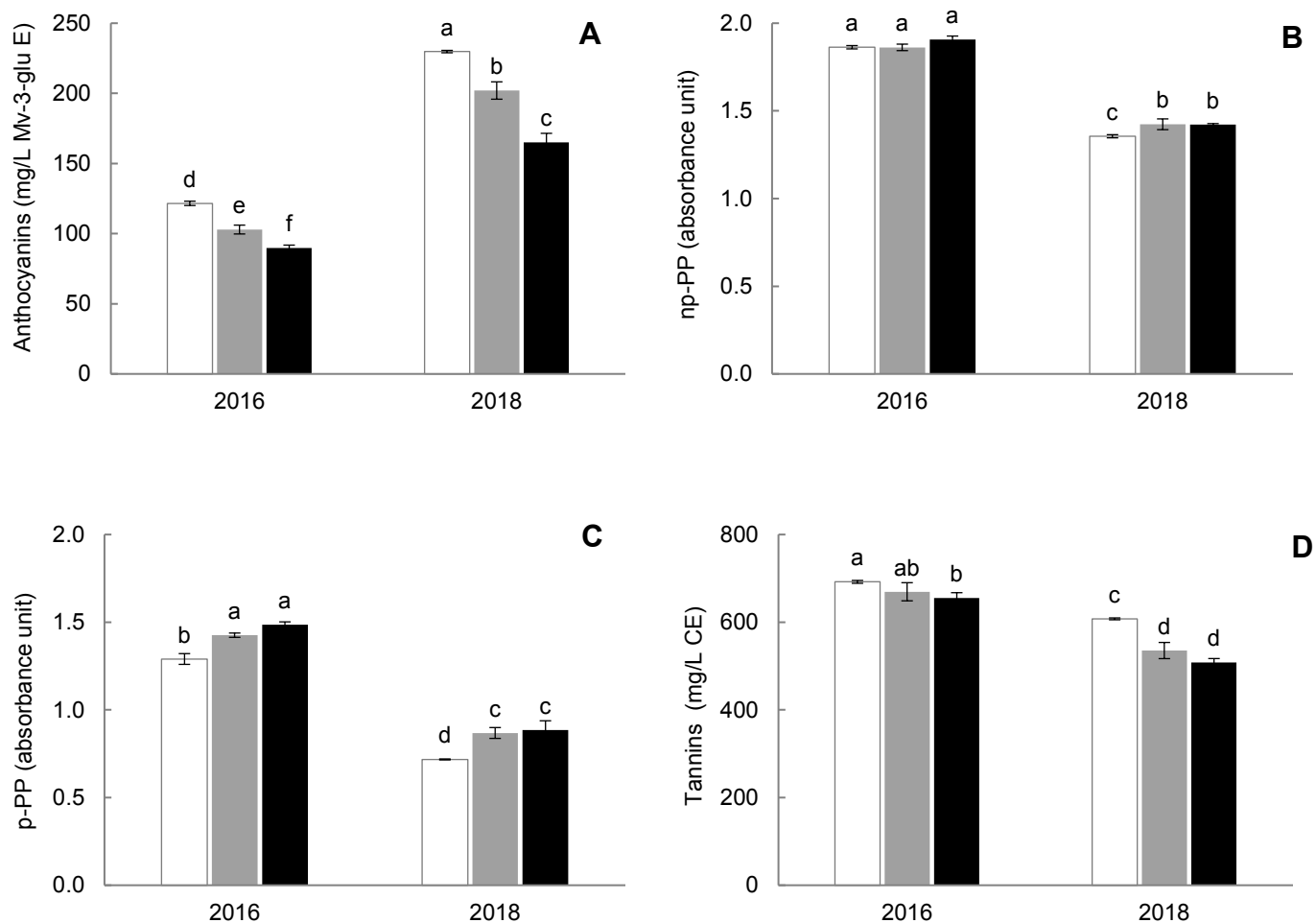


**Figure 1** Phenolic composition including total anthocyanins (**A**), non-precipitable polymeric pigments (np-PP; **B**), precipitable polymeric pigments (p-PP; **C**), and total tannins (**D**) of Cabernet Sauvignon wines at the various stages of storage at 35°C: no storage (□), 3 weeks (■), and 6 weeks (■). Results obtained by photometric assays (Harbertson et al. 2002, 2003, 2009, 2015). Means presented with standard deviation; n = 3. Means having the same letters are not significantly different at  $p \leq 0.05$ .

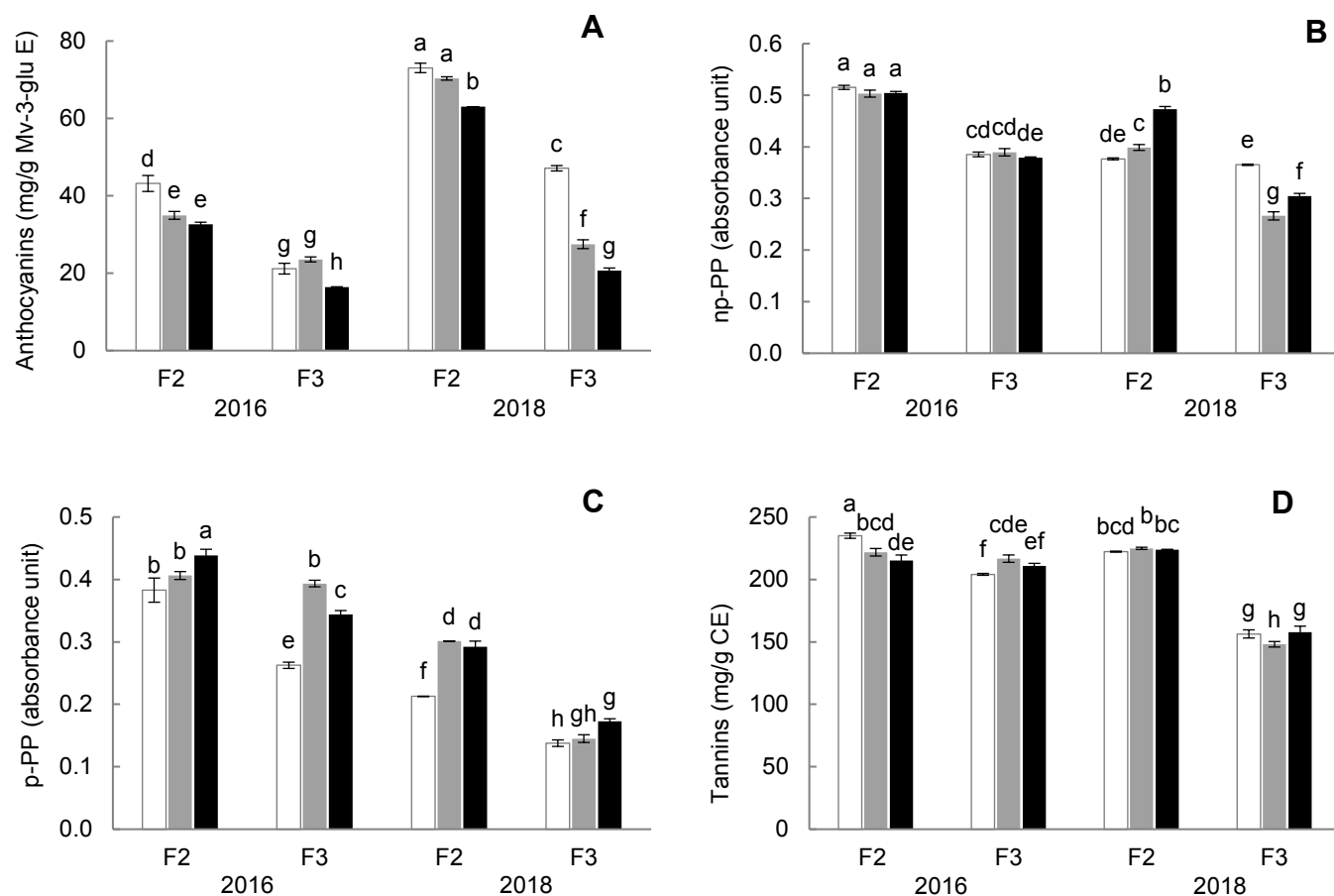


**Figure 2** Phenolic composition including total anthocyanins (A), non-precipitable polymeric pigments (np-PP; B), precipitable polymeric pigments (p-PP; C), and total tannins (D) of silica gel chromatography fraction 2 (F2) and fraction 3 (F3) of Cabernet Sauvignon XAD7 extracts at the various stages of storage at 35°C: no storage (□), 3 weeks (■), and 6 weeks (■). Results obtained by photometric assays (Harbertson et al. 2002, 2003, 2009, 2015). Means presented with standard deviation; n = 3. Means having the same letters are not significantly different at  $p \leq 0.05$ .

Figure 3

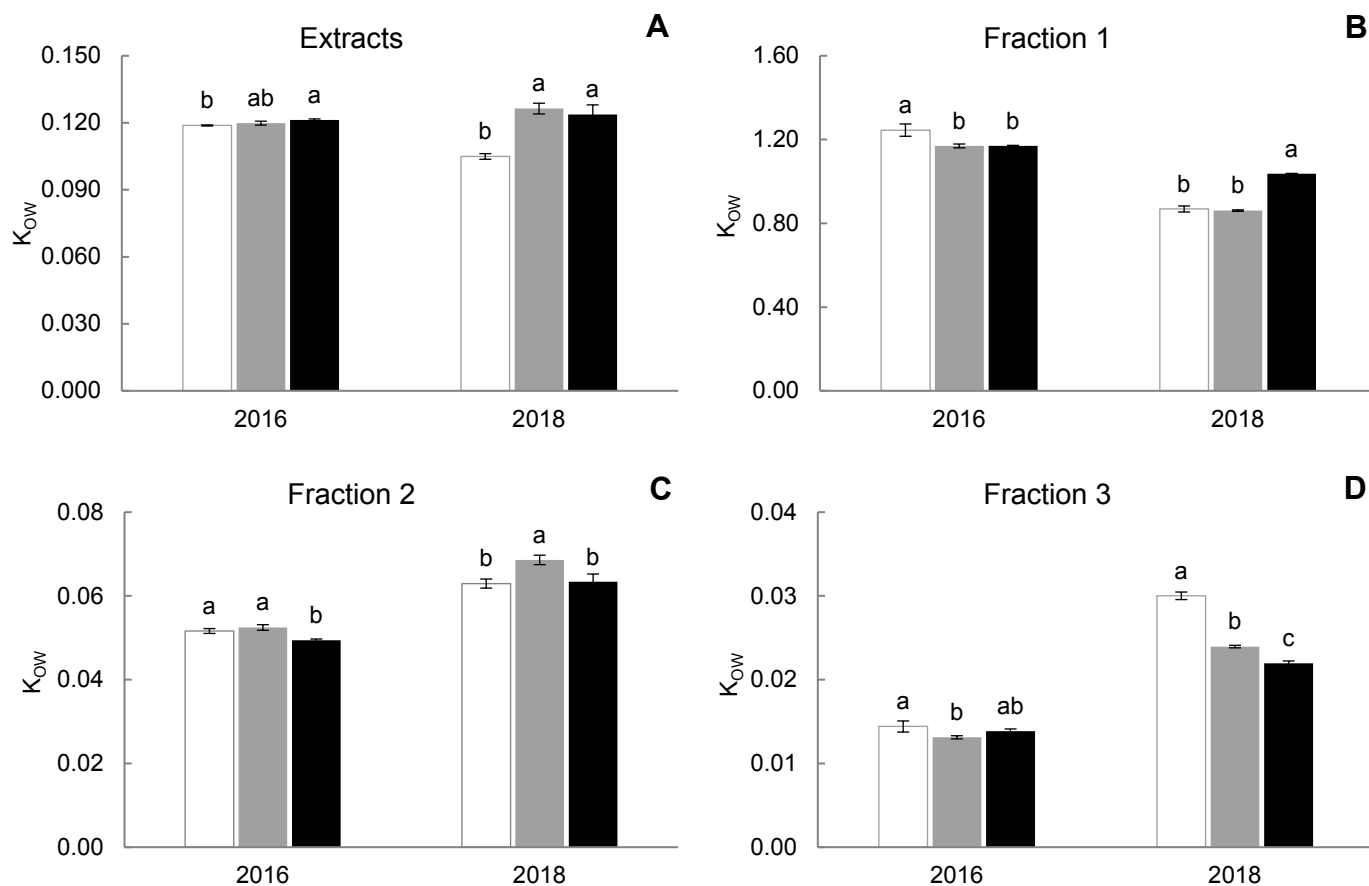


**Figure 3** Octanol water partitioning coefficients ( $K_{ow}$ ) of XAD7 extracts (A), and silica gel chromatography fraction 1 (B), fraction 2 (C), and fraction 3 (D) of Cabernet Sauvignon wines at the various stages of storage at 35°C: no storage (□), 3 weeks (■), and 6 weeks (■). Means presented with standard deviation;  $n = 3$ . Means within columns having the same letters are not significantly different at  $p \leq 0.05$ .

**Supplemental Table 1** Fourway-ANOVA of the astringency rating including vintage, storage, panelist, and replicate of the tasting showing that the vintage of the wines and the panelist have a significant impact on the astringency rating at  $p \leq 0.05$ .

Source	Degrees of freedom	Sum of squares	Mean of squares	F-value	p-value
Vintage	1	48.747	48.747	12.861	0.000
Storage	2	20.859	10.430	2.752	0.068
Panelist	13	100.143	7.703	2.032	0.023
Replicate	1	0.547	0.547	0.144	0.705

**Supplemental Table 2** Heat map of the low molecular phenolic composition of 2016 Cabernet Sauvignon wine fractions at the various stages of storage at 35°C determined with UHPLC-MS/MS. Means presented with mean standard deviation (mSD) for substance classes, n = 3.

Substance (mg/g)	Fraction 1			Fraction 2			Fraction 3		
	0	3	6	0	3	6	0	3	6
<i>Anthocyanins</i> ( $\pm 0.06$ mSD)									
Delphinidin-3-glucoside	n.d.	n.d.	n.d.	0.39	0.36	0.27	0.62	0.44	0.41
Cyanidin-3-glucoside	n.d.	n.d.	n.d.	0.07	0.06	0.05	0.06	0.03	0.03
Petunidin-3-glucoside	n.d.	n.d.	n.d.	0.92	0.78	0.62	0.73	0.56	0.50
peonidin-3-glucoside	n.d.	n.d.	n.d.	0.89	0.68	0.61	0.22	0.22	0.15
Malvidin-3-glucoside	n.d.	n.d.	n.d.	13.06	9.46	9.00	4.16	4.05	2.79
Delphinidin-3-(6-acetyl)glucoside	n.d.	n.d.	n.d.	0.09	0.09	0.06	0.18	0.12	0.11
Petunidin-3-O-(6-O-acetyl)glucoside	n.d.	n.d.	n.d.	0.28	0.23	0.18	0.23	0.16	0.14
Malvidin Formiat	n.d.	n.d.	n.d.	0.28	0.26	0.26	0.12	0.08	0.06
Peonidin 3-O-acetylglucoside	n.d.	n.d.	n.d.	0.40	0.28	0.24	0.07	0.07	0.04
Delphinidin-3-(p-coumaroyl)glucoside	n.d.	n.d.	n.d.	n.d.	n.d.	n.d.	n.d.	n.d.	n.d.
Malvidin-3-O-(6-O-acetyl)glucoside	n.d.	n.d.	n.d.	5.43	3.95	3.36	1.23	1.15	0.80
Petunidin-3-(p-coumaroyl)glucoside cis	n.d.	n.d.	n.d.	n.d.	n.d.	n.d.	0.04	n.d.	n.d.
Petunidin-3-(p-coumaroyl)glucoside trans	n.d.	n.d.	n.d.	0.06	0.05	0.04	n.d.	n.d.	n.d.
Malvidin-3-O-(6-O-p-coumaroyl)glucoside cis	n.d.	n.d.	n.d.	0.08	0.05	0.05	n.d.	n.d.	n.d.
Peonidin-3-(6"-p-coumaroyl)glucoside)	n.d.	n.d.	n.d.	0.14	0.10	0.09	n.d.	n.d.	n.d.
Malvidin-3-O-(6-O-p-coumaroyl)glucoside trans	n.d.	n.d.	n.d.	1.16	0.83	0.76	0.22	0.22	0.17
<i>Pyranoanthocyanins</i> ( $\pm 0.01$ mSD)									
Petunidin-3-glucoside pyruvate (Vitisin A)	n.d.	n.d.	n.d.	0.05	0.05	0.05	0.04	0.04	0.04
Peonidin-3-glucoside pyruvate (Vitisin A)	n.d.	n.d.	n.d.	0.05	0.05	0.05	n.d.	n.d.	n.d.
Malvidin-3-O-glucosid pyruvate (Vitisin A)	n.d.	n.d.	n.d.	0.23	0.20	0.20	0.10	0.11	0.11



Malvidin-3-O-acetylglucoside pyruvate (Vitisin A)	n.d.	n.d.	n.d.	0.16	0.15	0.16	n.d.	n.d.	n.d.
Malvidin-3-glucoside-vinyl-catechin	n.d.	n.d.	n.d.	0.06	0.05	0.06	n.d.	n.d.	n.d.
Mv-3-glc-4-vinylcatechol (Pinotin)	n.d.	n.d.	n.d.	0.50	0.49	0.59	0.23	0.28	0.29
Malvidin-3-glucoside-vinyl-epicatechin	n.d.	n.d.	n.d.	0.09	0.08	0.09	n.d.	n.d.	n.d.
Malvidin-3-glucoside-4-vinylphenol (Pinotin)	n.d.	n.d.	n.d.	0.53	0.84	0.55	0.13	0.32	0.23
<i>Anthocyanin flavanol adducts (±0.01 mSD)</i>									
Malvidin-3-glucoside-galocatechin	n.d.	n.d.	n.d.	0.23	0.21	0.20	0.06	0.05	0.04
Peonidin-3-glucoside-(epi)catechin	n.d.	n.d.	n.d.	0.08	0.08	0.07	n.d.	n.d.	n.d.
Malvidin-glucoside-(epi)catechin	n.d.	n.d.	n.d.	0.75	0.73	0.68	0.17	0.19	0.15
Malvedin-acetylglucoside-(epi)catechin	n.d.	n.d.	n.d.	0.13	0.12	0.11	n.d.	n.d.	n.d.
Malvidin-coumaroylglucoside-(epi)catechin	n.d.	n.d.	n.d.	0.06	0.06	0.05	n.d.	n.d.	n.d.
<i>Flavanols (±0.87 mSD)</i>									
Catechingallat	1.89	2.02	2.61	0.98	0.70	0.48	0.52	0.45	0.30
(-)-Galocatechin	7.57	6.08	9.67	0.71	0.92	0.64	0.18	0.15	0.15
Epicatechingallat	1.29	1.13	1.63	0.70	0.43	0.34	n.d.	n.d.	n.d.
(-)-Epigalocatechin	2.57	1.89	2.75	0.16	0.18	0.12	0.05	0.04	0.04
Catechin	48.55	38.99	48.28	3.31	4.11	2.47	1.02	0.96	0.85
Epicatechin	33.78	23.75	28.66	1.80	2.28	1.54	0.72	0.65	0.62
<i>Proanthocyanidins (±0.30 mSD)</i>									
Flavanol trimer	0.60	0.50	0.58	0.42	0.18	0.15	0.37	0.32	0.29
Flavanol dimer	12.59	11.04	14.65	3.60	2.59	1.94	0.99	0.96	0.78
Flavanol dimer	4.04	3.19	4.47	0.54	0.38	0.23	0.05	0.07	0.06
Flavanol trimer	1.31	1.31	1.86	0.71	0.44	0.35	0.09	0.08	0.07
Flavanol trimer	0.99	1.10	1.61	0.43	0.30	0.22	0.03	0.03	0.03
Flavanol dimer	2.74	1.93	2.33	0.23	0.17	0.11	n.d.	n.d.	n.d.
Flavanol trimer	0.85	0.90	1.25	0.42	0.25	0.20	n.d.	n.d.	n.d.

Flavanol dimer	13.85	10.12	13.80	2.23	1.59	1.17	0.58	0.56	0.46
Flavanol dimer gallat	0.07	0.18	0.23	0.16	0.15	0.13	n.d.	n.d.	n.d.
Flavanol dimer gallat	0.02	0.06	0.09	0.09	0.09	0.07	n.d.	n.d.	n.d.
Flavanol trimer	1.69	1.54	2.08	0.52	0.32	0.22	0.07	0.06	0.05
<i>Flavonols (±0.23 mSD)</i>									
Dihydromyricetin-3-rhamnoside	0.10	0.14	0.19	0.17	0.15	0.12	n.d.	n.d.	n.d.
Myricetin-3-glucuronide	0.13	0.18	0.18	2.00	1.98	2.00	n.d.	n.d.	n.d.
Quercetin-3-O-glucuronide	0.91	1.23	1.19	4.99	3.95	4.31	0.60	0.50	0.57
Laricitrin-3-galactoside	n.d.	n.d.	n.d.	0.22	0.14	0.13	n.d.	n.d.	n.d.
Syringetin-3-glucoside	0.03	0.05	0.05	3.01	2.16	2.04	0.46	0.41	0.44
<i>Benzoic acids (±1.49 mSD)</i>									
Gallic acid	62.69	53.79	70.25	4.05	4.13	3.77	0.55	0.61	0.85
Vanillic acid	1.81	1.31	1.62	n.d.	n.d.	n.d.	n.d.	n.d.	n.d.
<i>Hydroxycinnamic acids (±0.35 mSD)</i>									
Cis-Caftaric acid	0.97	1.38	1.16	0.29	0.20	0.15	n.d.	n.d.	n.d.
Cis-Caffeic acid	6.16	5.17	5.77	2.42	2.03	1.89	n.d.	n.d.	n.d.
Trans-Caftaric acid	6.92	5.73	6.74	2.34	1.85	1.81	0.12	0.12	0.14
Hydroxy-caffeic acid dimer isomer	1.73	1.56	1.39	0.68	0.59	0.61	n.d.	n.d.	n.d.
Ferulic acid	0.85	0.55	0.83	n.d.	n.d.	n.d.	n.d.	n.d.	n.d.
cis-Coutaric acid	1.94	1.52	1.74	0.43	0.33	0.30	n.d.	n.d.	n.d.
p-Coumaric acid	13.64	11.81	13.69	n.d.	n.d.	n.d.	n.d.	n.d.	n.d.
trans-Coutaric acid	7.00	5.41	8.06	1.09	0.88	0.80	0.06	0.06	0.06
Trans-Caffeic acid	18.10	13.51	17.13	0.26	0.26	0.20	n.d.	n.d.	n.d.
cis-Ethylcaffeic acid	2.72	2.25	2.28	n.d.	n.d.	n.d.	n.d.	n.d.	n.d.

**Supplemental Table 3** Heat map of the low molecular phenolic composition of 2018 Cabernet Sauvignon wine fractions at the various stages of storage at 35°C determined with UHPLC-MS/MS. Means presented with mean standard deviation (mSD) for substance classes, n = 3.

Substance (mg/g)	Fraction 1			Fraction 2			Fraction 3		
	0	3	6	0	3	6	0	3	6
<i>Anthocyanins</i> ( $\pm 0.06$ mSD)									
Delphinidin-3-glucoside	n.d.	n.d.	n.d.	0.62	0.54	0.44	2.73	1.09	0.94
Cyanidin-3-glucoside	n.d.	n.d.	n.d.	0.13	0.11	0.09	0.32	0.12	0.08
Petunidin-3-glucoside	n.d.	n.d.	n.d.	2.20	1.81	1.49	5.12	1.92	1.41
peonidin-3-glucoside	n.d.	0.05	n.d.	3.66	2.82	2.29	1.14	0.66	0.57
Malvidin-3-glucoside	0.06	0.37	0.03	30.00	26.71	22.49	12.78	8.34	7.99
Delphinidin-3-(6-acetyl)glucoside	n.d.	n.d.	n.d.	0.10	0.08	0.07	0.55	0.21	0.19
Petunidin-3-O-(6-O-acetyl)glucoside	n.d.	n.d.	n.d.	0.45	0.36	0.30	1.06	0.42	0.30
Malvidin Formiat	n.d.	n.d.	n.d.	0.82	1.00	0.65	0.23	0.15	0.13
Peonidin 3-O-acetylglucoside	0.03	0.04	n.d.	1.23	0.95	0.75	0.32	0.20	0.15
Delphinidin-3-(p-coumaroyl)glucoside	n.d.	n.d.	n.d.	0.13	0.11	0.09	0.42	0.19	0.12
Malvidin-3-O-(6-O-acetyl)glucoside	0.20	0.31	0.17	13.69	11.25	9.36	3.73	2.83	2.18
Petunidin-3-(p-coumaroyl)glucoside cis	n.d.	n.d.	n.d.	n.d.	n.d.	n.d.	0.67	0.29	0.17
Petunidin-3-(p-coumaroyl)glucoside trans	n.d.	n.d.	n.d.	0.44	0.33	0.27	n.d.	n.d.	n.d.
Malvidin-3-O-(6-O-p-coumaroyl)glucoside cis	n.d.	n.d.	n.d.	0.59	0.39	0.29	0.13	0.10	0.06
Peonidin-3-(6"-p-coumaroyl)glucoside)	n.d.	n.d.	n.d.	0.89	0.77	0.58	0.20	0.15	0.10
Malvidin-3-O-(6-O-p-coumaroyl)glucoside trans	n.d.	n.d.	n.d.	6.99	5.74	4.56	1.50	1.21	0.88
<i>Pyranoanthocyanins</i> ( $\pm 0.01$ mSD)									
Petunidin-3-glucoside pyruvate (Vitisin A)	n.d.	n.d.	n.d.	0.04	0.04	0.03	0.13	0.04	0.03
Peonidin-3-glucoside pyruvate (Vitisin A)	n.d.	n.d.	n.d.	0.04	0.05	0.04	n.d.	n.d.	n.d.
Malvidin-3-O-glucosid pyruvate (Vitisin A)	n.d.	n.d.	n.d.	0.22	0.19	0.19	0.09	0.09	0.08

Malvidin-3-O-acetylglucoside pyruvate (Vitisin A)	n.d.	n.d.	n.d.	0.15	0.15	0.14	n.d.	n.d.	n.d.
Malvidin-3-glucoside-vinyl-catechin	n.d.	n.d.	n.d.	0.05	0.05	0.05	n.d.	n.d.	n.d.
Mv-3-glc-4-vinylcatechol (Pinotin)	n.d.	n.d.	n.d.	0.09	0.15	0.18	0.19	0.11	0.09
Malvidin-3-glucoside-vinyl-epicatechin	n.d.	n.d.	n.d.	0.08	0.08	0.07	n.d.	n.d.	n.d.
Malvidin-3-glucoside-4-vinylphenol (Pinotin)	n.d.	n.d.	n.d.	0.69	1.15	0.75	0.47	0.15	0.20
<i>Anthocyanin flavanol adducts (±0.01 mSD)</i>									
Malvidin-3-glucoside-gallocatechin	n.d.	n.d.	n.d.	0.28	0.32	0.29	0.11	0.07	0.06
Peonidin-3-glucoside-(epi)catechin	n.d.	n.d.	n.d.	0.14	0.16	0.14	0.07	0.04	0.04
Malvidin-glucoside-(epi)catechin	n.d.	n.d.	n.d.	0.86	1.07	0.91	0.36	0.24	0.25
Malvedin-acetylglucoside-(epi)catechin	n.d.	n.d.	n.d.	0.19	0.21	0.18	0.05	0.04	0.04
Malvidin-coumaroylglucoside-(epi)catechin	n.d.	n.d.	n.d.	0.16	0.20	0.17	0.05	0.04	0.04
<i>Flavanols (±0.87 mSD)</i>									
Catechingallat	3.26	3.27	3.26	1.55	1.44	1.05	0.47	0.97	0.71
(-)-Gallocatechin	9.01	6.67	8.16	0.94	1.01	0.70	0.23	0.14	0.13
Epicatechingallat	2.38	2.03	1.87	1.07	0.99	0.67	n.d.	n.d.	n.d.
(-)-Epigallocatechin	2.79	2.55	2.69	0.18	0.21	0.15	0.06	0.04	0.04
Catechin	56.66	51.39	55.98	3.87	4.33	3.59	1.32	0.90	0.86
Epicatechin	47.43	36.74	39.62	2.62	2.45	1.90	1.12	0.67	0.64
<i>Proanthocyanidins (±0.30 mSD)</i>									
Flavanol trimer	1.32	1.41	1.04	0.87	0.83	0.44	0.35	0.37	0.38
Flavanol dimer	20.22	18.91	18.54	6.49	6.96	4.43	1.98	1.01	1.04
Flavanol dimer	6.97	5.98	5.32	1.18	1.13	0.67	0.13	0.06	0.06
Flavanol trimer	3.36	2.87	2.81	1.50	1.31	0.87	0.22	0.09	0.09
Flavanol trimer	2.47	2.27	2.06	0.87	0.81	0.65	0.08	0.05	0.04
Flavanol dimer	5.45	3.90	3.98	0.62	0.54	0.29	0.08	0.06	0.07
Flavanol trimer	1.74	1.56	1.51	0.67	0.64	0.52	n.d.	n.d.	n.d.

Flavanol dimer	19.64	17.54	17.33	4.44	3.86	2.65	1.18	0.64	0.60
Flavanol dimer gallat	0.25	0.44	0.39	0.34	0.37	0.30	0.06	0.03	0.03
Flavanol dimer gallat	0.10	0.19	0.16	0.18	0.20	0.18	n.d.	n.d.	n.d.
Flavanol trimer	3.91	3.35	3.22	1.28	1.04	0.69	0.20	0.08	0.08
<i>Flavonols (±0.23 mSD)</i>									
Dihydromyricetin-3-rhamnoside	0.05	0.07	0.07	0.09	0.08	0.06	n.d.	n.d.	n.d.
Myricetin-3-glucuronide	0.30	0.43	0.26	2.70	2.18	2.03	n.d.	n.d.	n.d.
Quercetin-3-O-glucuronide	11.28	11.22	8.32	25.36	22.56	19.87	6.31	4.86	3.98
Laricitrin-3-galactoside	0.03	0.14	0.03	0.90	0.79	0.62	0.20	0.12	0.10
Syringetin-3-glucoside	0.08	0.57	0.10	3.64	3.49	2.80	0.85	0.68	0.55
<i>Benzoic acids (±1.49 mSD)</i>									
Gallic acid	67.91	65.59	66.14	4.68	3.96	3.12	1.85	0.63	0.74
Vanillic acid	3.05	3.19	3.10	n.d.	n.d.	n.d.	n.d.	n.d.	n.d.
<i>Hydroxycinnamic acids (±0.35 mSD)</i>									
Cis-Caftaric acid	2.70	1.16	0.62	0.54	0.41	0.18	0.04	0.08	0.04
Cis-Caffeic acid	8.85	9.32	10.49	2.55	2.73	2.15	n.d.	n.d.	n.d.
Trans-Caftaric acid	10.72	10.68	11.94	2.90	2.90	2.34	0.47	0.22	0.22
Hydroxy-caffeic acid dimer isomer	1.55	1.90	1.65	0.46	0.59	0.43	n.d.	n.d.	n.d.
Ferulic acid	0.95	0.95	0.99	n.d.	n.d.	n.d.	n.d.	n.d.	n.d.
cis-Coutaric acid	3.33	2.72	2.68	0.65	0.64	0.38	0.08	0.04	0.04
p-Coumaric acid	14.11	14.46	14.75	n.d.	n.d.	n.d.	n.d.	n.d.	n.d.
trans-Coutaric acid	9.27	7.73	8.93	1.10	1.05	0.75	0.15	0.07	0.07
Trans-Caffeic acid	15.89	15.10	15.00	0.16	0.09	0.08	n.d.	n.d.	n.d.
cis-Ethylcaffeic acid	2.33	2.44	2.40	n.d.	n.d.	n.d.	n.d.	n.d.	n.d.